Journal of Crystal Growth 474 (2017) 110–120

Contents lists available at ScienceDirect

Journal of Crystal Growth

journal homepage: www.elsevier.com/locate/jcrysgro

Thermal equilibrium concentration of intrinsic point defects in heavily doped silicon crystals - Theoretical study of formation energy and formation entropy in area of influence of dopant atoms-

K. Kobayashi[a,*], S. Yamaoka[a], K. Sueoka[a], J. Vanhellemont[b]

[a] Department of Communication Engineering, Okayama Prefectural University, 111 Kuboki, Soja, Okayama 719-1197, Japan
[b] Department of Solid State Sciences, Ghent University, Krijgslaan 281 S1, Gent B-9000, Belgium

ARTICLE INFO

Keywords:
Intrinsic point defect
Silicon
Thermal equilibrium concentration
Density functional theory
Doping

ABSTRACT

It is well known that p-type, neutral and n-type dopants affect the intrinsic point defect (vacancy *V* and self-interstitial *I*) behavior in single crystal Si. By the interaction with *V* and/or *I*, (1) growing Si crystals become more *V*- or *I*-rich, (2) oxygen precipitation is enhanced or retarded, and (3) dopant diffusion is enhanced or retarded, depending on the type and concentration of dopant atoms. Since these interactions affect a wide range of Si properties ranging from as-grown crystal quality to LSI performance, numerical simulations are used to predict and to control the behavior of both dopant atoms and intrinsic point defects. In most cases, the thermal equilibrium concentrations of dopant-point defect pairs are evaluated using the mass action law by taking only the binding energy of closest pair to each other into account. The impacts of dopant atoms on the formation of *V* and *I* more distant than 1st neighbor and on the change of formation entropy are usually neglected. In this study, we have evaluated the thermal equilibrium concentrations of intrinsic point defects in heavily doped Si crystals. Density functional theory (DFT) calculations were performed to obtain the formation energy (E_f) of the uncharged *V* and *I* at all sites in a 64-atom supercell around a substitutional p-type (B, Ga, In, and Tl), neutral (C, Ge, and Sn) and n-type (P, As, and Sb) dopant atom. The formation (vibration) entropies (S_f) of free *I, V* and *I, V* at 1st neighboring site from B, C, Sn, P and As atoms were also calculated with the linear response method. The dependences of the thermal equilibrium concentrations of trapped and total intrinsic point defects (sum of free *I* or *V* and *I* or *V* trapped with dopant atoms) on the concentrations of B, C, Sn, P and As in Si were obtained. Furthermore, the present evaluations well explain the experimental results of the so-called "Voronkov criterion" in B and C doped Si, and also the observed dopant dependent void sizes in P and As doped Si crystals. The expressions obtained in the present work are very useful for the numerical simulation of grown-in defect behavior, oxygen precipitation and dopant diffusion in heavily doped Si. DFT calculations also showed that Coulomb interaction reaches approximately 30 Å from p (n)-type dopant atoms to *I* (*V*) in Si.

1. Introduction

It is well known that p-type, neutral and n-type dopants affect the intrinsic point defect (vacancy *V* and self-interstitial *I*) behavior in single crystal Si. By the interaction with *V* and/or *I*, (1) growing Si crystals become more *V*- or *I*-rich [3,5,14,20,2,23], (2) oxygen precipitation is enhanced or retarded [20,18], and (3) dopant diffusion is enhanced or retarded [7,11], depending on the type and concentration of dopant atoms. In case (1), a reduction of the radius of the oxidation induced stacking fault (OSF) ring in CZ-Si was observed in case of B doping higher than ~1×10^{18} B cm^{-3}[5]. High concentrations of P, As, or Sb doping make the crystal more *V*-rich [14]. In case (2), oxygen precipitation is enhanced by B or C doping [18] while it is retarded by P or As doping [20]. In case (3), B diffusion is mediated by self-interstitials [7] while Sb diffusion is mediated by vacancies in Si [11].

Since these interactions affect a wide range of Si properties ranging from as-grown crystal quality to LSI performance, numerical simulations are used to predict and to control the behaviors of both dopant atoms and intrinsic point defects [14,8]. In most cases, the thermal equilibrium concentrations of dopant-point defect pairs are evaluated using mass action law by taking only the binding energy of the closest pair to each other into account [14]. The impacts of dopant atoms on the formation of *V* and *I* more distant than 1st neighbor and on the change of formation entropy are usually neglected. In a previous study

* Corresponding author.
E-mail address: kjkobayashi458@gmail.com (K. Kobayashi).

http://dx.doi.org/10.1016/j.jcrysgro.2016.11.098
Received 14 January 2016; Received in revised form 18 November 2016; Accepted 24 November 2016
Available online 25 November 2016

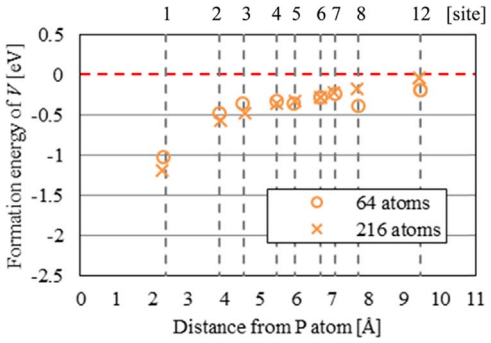

Fig. 1. (color online) Comparison of the calculated change of V formation energy E_f^V at each site around the central P atom in 64-atom and 216-atom Si supercells. The dotted lines at 1st to 8th, and 12th site indicate the distance from P atom before ionic coordinates are relaxed.

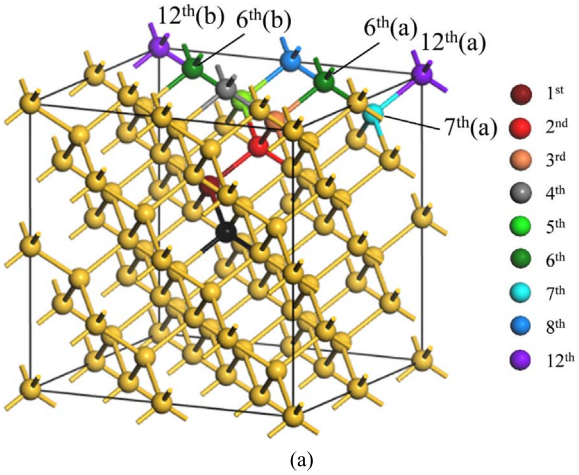

(a)

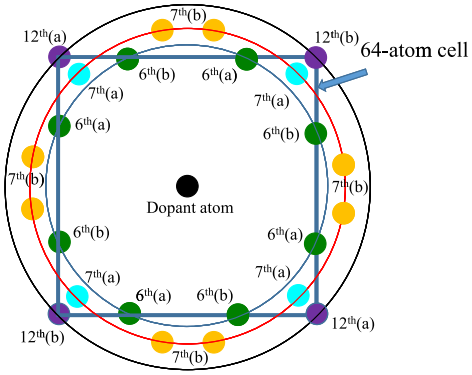

(b)

Fig. 2. (color online) (a) 64-atom calculation cell with V sites classified according to the distance from the dopant atom in the center (black). (b) Supplementary illustration for 6th, 7th and 12th sites on circles with dopant atom (black) at the center and 64-atom supercell.

of the authors [17], an appropriate model of V and I behavior in a growing single crystal Si was proposed based on density functional theory (DFT) calculations of the formation energy (E_f) of V and I up to 5th neighboring sites from the dopant atom. To understand the dopant impact more precisely, even more distant sites should be considered as the E_f of V (I) at 5th site from n-type (p-type) dopant are still decreasing. Also the change of formation (vibration) entropies of V and I should be considered.

In this study, we have evaluated the thermal equilibrium concentrations of intrinsic point defects in heavily doped Si crystals. DFT calculations were performed to obtain E_f of the uncharged V and I at all

Table 1
Distance and coordination number of each V site around a central dopant atom before optimization of geometry in a Si 64-atom supercell with cell size of 10.937 Å.

No. V site from dopant atom	Distance from dopant atom (Å)	Coordination number
1st	2.37	4
2nd	3.87	12
3rd	4.53	12
4th	5.47	6
5th	5.96	12
6th (a)	6.69	12
6th (b)	6.69	12
7th	7.10	4
8th	7.73	12
12th (a)	9.40	4
12th (b)	9.40	4

sites in a 64-atom supercell around the substitutional p-type (B, Ga, In, and Tl), neutral (C, Ge, and Sn) and n-type (P, As, and Sb) dopant atoms. The formation entropies (S_f) of free I, V and I, V at 1st neighboring site from B, C, Sn, P and As atoms were also calculated with the linear response method. The dependences of the thermal equilibrium concentrations of trapped and total point defects (sum of free I or V and I or V trapped with dopant atoms) on the concentrations of B, C, Sn, P and As in Si are obtained. Furthermore, the experimental results of so-called "Voronkov criterion" in B and C doped Si, and also the observed void sizes in P and As doped Si crystals are explained. The expressions obtained in the present work are very useful for the numerical simulations of grown-in defect behavior, oxygen precipitation and dopant diffusion in heavily doped Si. The maximum distances of Coulomb interaction from p (n)-type dopant atoms to I (V) are also clarified.

2. Calculation details

DFT calculations were performed within the generalized gradient approximation (GGA) for electron exchange and correlation, using the CAmbridge Serial Total Energy Package (CASTEP) code [1]. The wave functions were expanded with plane waves, and the ultra-soft pseudopotential method [22] was used to reduce the number of plane waves. The cut-off energy was 340 eV. The expression proposed by Perdew et al. [15] was used for the exchange-correlation energy in the GGA. Density mixing [9] was used to optimize the electronic structure and Broyden Fletcher Goldfarb Shanno (BFGS) geometry optimization [6] was used to optimize the atomic configurations. The convergence condition to optimize the electronic structure was set to a change in total energy that was smaller than 5×10^{-7} eV/atom. The convergence conditions to optimize the geometry were set to a change in total energy that was smaller than 5×10^{-6} eV/atom, atomic force that was smaller than 0.001 eV/Å, and stress in the cell that was smaller than 0.001 GPa.

In the present study, we considered only neutral intrinsic point defects. The cell size of a perfect 64-atom Si supercell after its geometry optimization was 10.937 Å. Periodic boundary conditions were used to calculate perfect and defect-containing Si crystals. k-point sampling was performed at 2×2×2 special points in a Monkhorst-Pack grid [12]. In a single crystal Si, the thermal equilibrium concentrations of V and I, even near melting temperature, are well below 5×10^{15} cm^{-3}[14]. For such low concentration, the calculation cell should be surrounded by perfect cells. Therefore, the calculations for the dopant and/or intrinsic point defects were performed by using a cubic supercell with the same cell size as for perfect crystals. Preliminary calculations were performed to confirm the reliability of a calculation cell of 64-atoms. Fig. 1 shows the comparison of the results obtained for 64-atom and 216-atom supercells for the change of V formation energy E_f at 1st to 8th, and 12th site from the P atom doped in Si crystal. The dotted black lines at

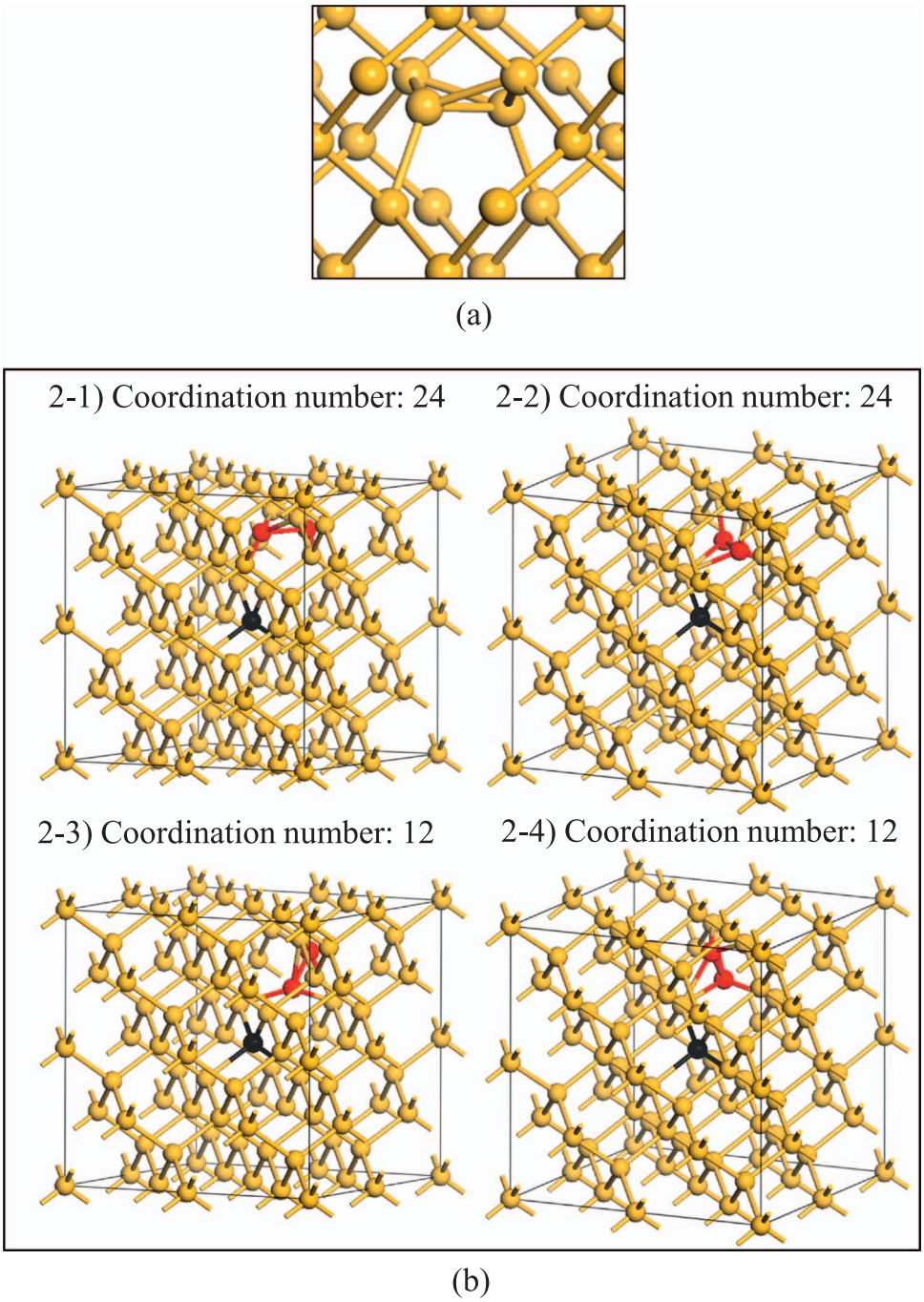

Fig. 3. (color online) (a) Atomic configuration of [110] dumbbell site. (b) Four different atomic configurations of D-site (red) at 2nd site from the dopant atom (black).

1st to 8th, and 12th site indicate the distance from the P atom before ionic coordinates are relaxed. The very small difference between 64 and 216-atom supercells indicates that the 64-atom supercell is large enough for the calculations of *V* and *I* with low concentrations in Si.

Fig. 2(a) shows the calculation model, *i.e.*, a 64-atom cubic cell, with vacancy sites classified according to the distance from the dopant atom in the center of the cell. The neighboring sites in the 64-atom cell are illustrated in Fig. 2(b). In the 64-atom model, there are 1st, 2nd, ..., 8th and 12th neighboring sites. Here, we note that the 6th site is classified into two sites (6th(a) and 6th(b)) for which the atomic configurations differ from each other. For the 7th site, there are also two different atomic configurations but only one configuration (7th(a)) is included in the 64-atom cell as shown in Fig. 2(b). For the 12th site, two different atomic configurations (12th(a) and 12th(b)) exist but these two configurations are dealt with as the same ones by the periodic boundary conditions. Table 1 summarizes the distance and the coordination number of each *V* site around a dopant atom before the optimization of the geometry of the 64-atom Si supercell. The 9th, 10th, and 11th sites are not included in the 64-atom model. To avoid the adverse effect of cell constraint, pairs of the dopant and *V* at 3rd ~ 12th sites are moved to the central region of the 64-atom model.

The formation energies E_f^V and $E_f^{V\ (doped)}$ of *V* in perfect and doped Si crystals, respectively, are obtained from

$$E_f^V = E_{tot}[Si_{63}V_1] - 63E_{tot}[Si_{64}]/64 \quad (1a)$$

and

$$E_f^{V\ (doped)} = E_{tot}[Si_{62}D_1V_1] - E_{tot}[Si_{63}D_1] + E_{tot}[Si_{64}]/64 \quad (1b)$$

Here, $E_{tot}[Si_{63}V_1]$ and $E_{tot}[Si_{64}]$ correspond with the total energies of

Table 2
Coordination number of each D-site around a central dopant atom in a Si 64-atom supercell.

No. of D-site from dopant atom	Numbering of independent site	Coordination number
0		12
1st	1–1	12
	1–2	12
2nd	2–1	24
	2–2	24
	2–3	12
	2–4	12
3rd	3–1	12
	3–2	24
	3–3	24
	3–4	12
4th	4–1	6
	4–2	24
	4–3	6
5th	5–1	24
	5–2	12
	5–3	12
	5–4	24
6th(a)	6(a)–1	12
	6(a)–2	24
	6(a)–3	24
	6(a)–4	12
6th(b)	6(b)–1	12
	6(b)–2	24
	6(b)–3	24
	6(b)–4	12
7th(a)	7–1	12
	7–2	12
8th	8–1	24
	8–2	12
	8–3	12
	8–4	24
12th(a)	12(a)–1	12
	12(a)–2	12
12th(b)	12(b)–1	12
	12(b)–2	12

the cell including one V and of the perfect Si cell, respectively. $E_{tot}[Si_{62}D_1V_1]$ is the total energy of the cell including one dopant atom (D) and one V, and $E_{tot}[Si_{63}D_1]$ is that including only one dopant atom.

The formation (vibration) entropies (S_f) of free V and V at 1st neighboring site from Sn, P and As atoms were calculated with the linear response method [4].

For the self-interstitial I, the [110] dumbbell (D)-site has the lowest energetic configuration for neutral self-interstitials while for positively charged self-interstitials it is the tetrahedral (T)-site [25]. Therefore, we considered both D- and T-sites around dopant atoms. In D-site, two Si atoms (one is I, and the other is a Si lattice atom) occupy near one lattice site as shown in Fig. 3(a). Each [110] D-site has 6 at. configurations at each site. There are 36 independent atomic configurations containing the dopant-I [110] dumbbell around the dopant atom in the center of a 64-atom supercell. Table 2 summarizes the coordination number of each D-site around a dopant atom. The coordination numbers at each site were counted taking the position and the direction of [110] Si-Si dumbbell into account. Dopant and I complex is indicated as 0th site. Four different atomic configurations at 2nd site from the dopant atom are shown in Fig. 3(b) as an example.

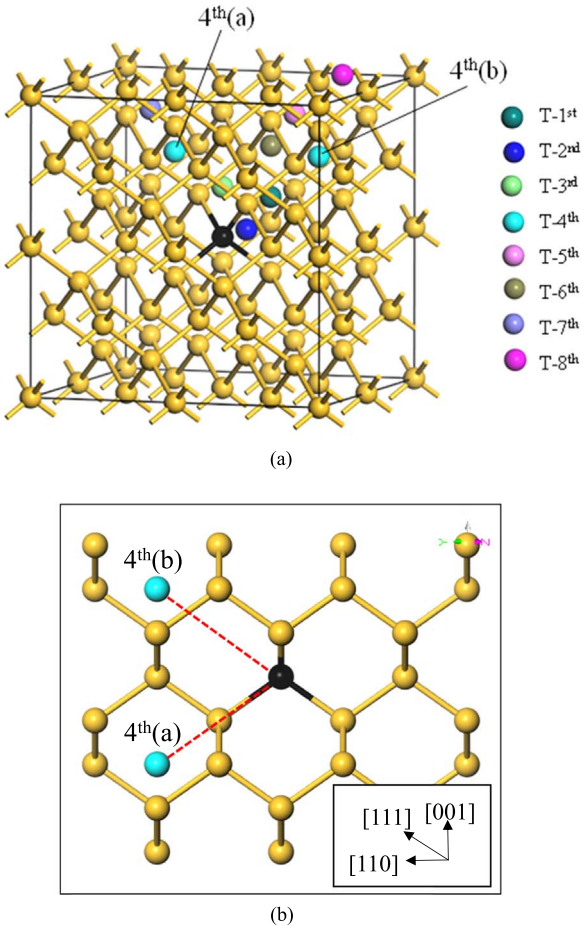

Fig. 4. (color online) (a) 64-atom calculation cell with T-sites of I classified according to the distance from the dopant atom in the center (black). (b) Atomic configurations of 4th(a) and 4th(b) sites. Note that one Si atom exists between I at 4th(a) T-site and dopant atom, while no Si atoms exist between I at 4th(b) T-site and dopant atom.

Table 3
Distance and coordination number of each T-site around a dopant atom before optimization of geometry in a Si 64-atom supercell with cell size of 10.937 Å.

No. of T-site from dopant atom	Distance from the dopant atom (Å)	Coordination number
1st	2.37	4
2nd	2.73	6
3rd	4.53	12
4th(a)	4.74	4
4th(b)	4.74	4
5th	5.96	12
6th	6.11	24
7th(a)	7.10	4
8th	8.10	24

Fig. 4(a) shows the calculation model with the T-sites classified according to the distance from the dopant atom. In the 64-atom model, there are 1st, 2nd, ..., and 8th neighboring sites. The 4th T-site is classified into two sites (4th(a) and 4th(b)) for which the atomic configurations differ from each other. One Si atom exists between I at 4th(a) of T-site and dopant atom, while no Si atoms exist between I at 4th(b) of T-site and dopant atom as shown in Fig. 4(b). For the 7th site, there are also two different atomic configurations but only one configuration (7th(a) site) is again included in the 64-atom cell. Table 3 summarizes the distance and the coordination number of each T-site around the dopant atom before the optimization of the geometry in a Si 64-atom supercell.

The formation energies E_f^I and $E_f^{I\,(doped)}$ of I in perfect and doped

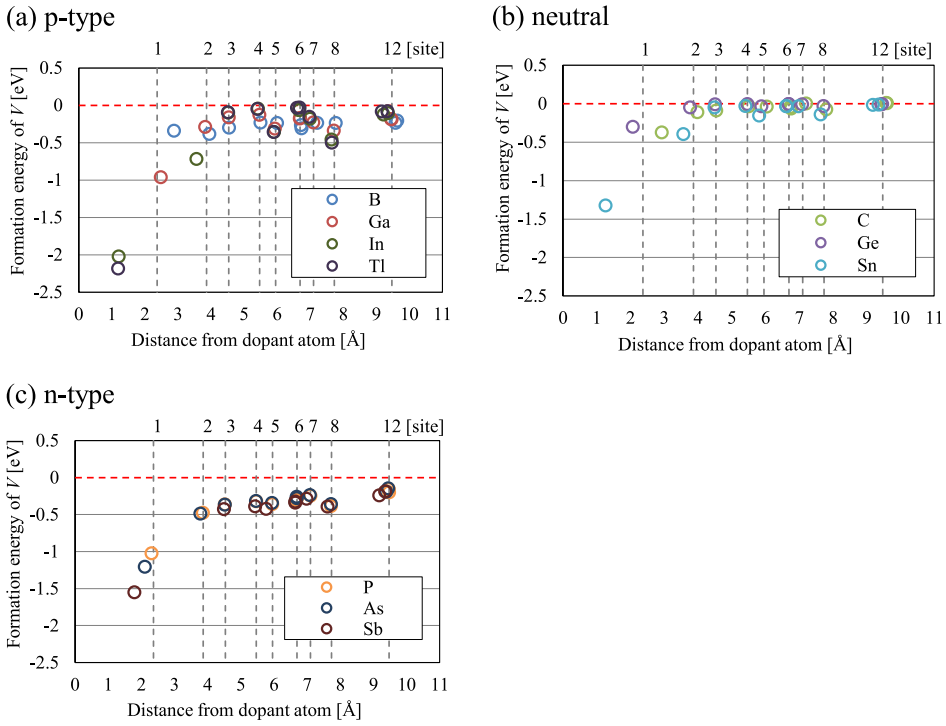

Fig. 5. (color online) Dependence of change in V formation energy (ΔE_f^V) from that in perfect Si crystal upon the distance from (a) p-type, (b) neutral, and (c) n-type dopant atoms. The dotted lines from 1st to 8th, and 12th site indicate the distance from dopant atom before ionic coordinates are relaxed.

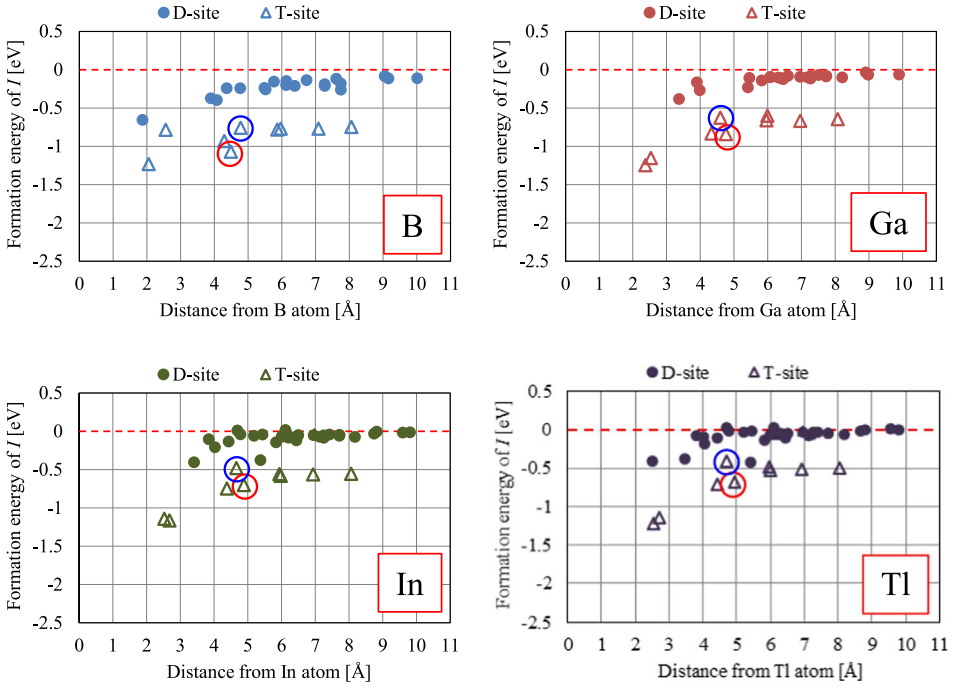

Fig. 6. (color online) Dependence of change in I formation energy (ΔE_f^I) at D-site and T-site compared to that in an undoped Si crystal upon the distance from the p-type dopant atom in the center. The data at 4th(a) (4th(b)) at T-site is shown with red (blue) circle.

Si crystals, respectively, are obtained from

$$E_f^I = E_{tot}[Si_{64}I_1] - 65E_{tot}[Si_{64}]/64 \quad (2a)$$

and

$$E_f^{I(doped)} = E_{tot}[Si_{63}D_1I_1] - E_{tot}[Si_{63}D_1] + E_{tot}[Si_{64}]/64 \quad (2b)$$

Here, $E_{tot}[Si_{63}I_1]$ and $E_{tot}[Si_{64}]$ correspond with the total energies of the cell including one I and of the perfect cell, respectively. $E_{tot}[Si_{62}D_1I_1]$ is the total energy of the cell including one dopant atom (D) and one I, and $E_{tot}[Si_{63}D_1]$ is that including only one dopant atom.

The formation (vibration) entropies (S_f) of free I and I at 1st neighboring site from C and B atoms were calculated with the linear response method [4].

The maximum distances of Coulomb interaction from p (n)-type dopant atoms to I (V) were evaluated by using rectangular models of 128, 192, 256, and 320 atoms elongated in the [100] direction. The calculation detail and results are mentioned in Section 3.3.

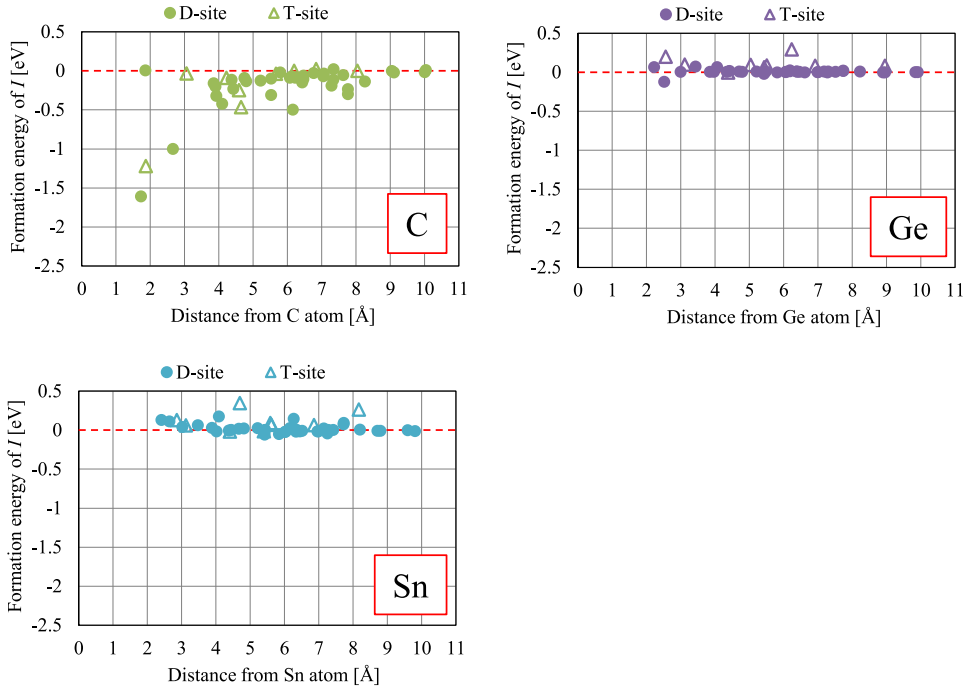

Fig. 7. (color online) Dependence of change in I formation energy (ΔE_f^I) at D-site and T-site compared to that in an undoped Si crystal upon the distance from the neutral dopant atom in the center.

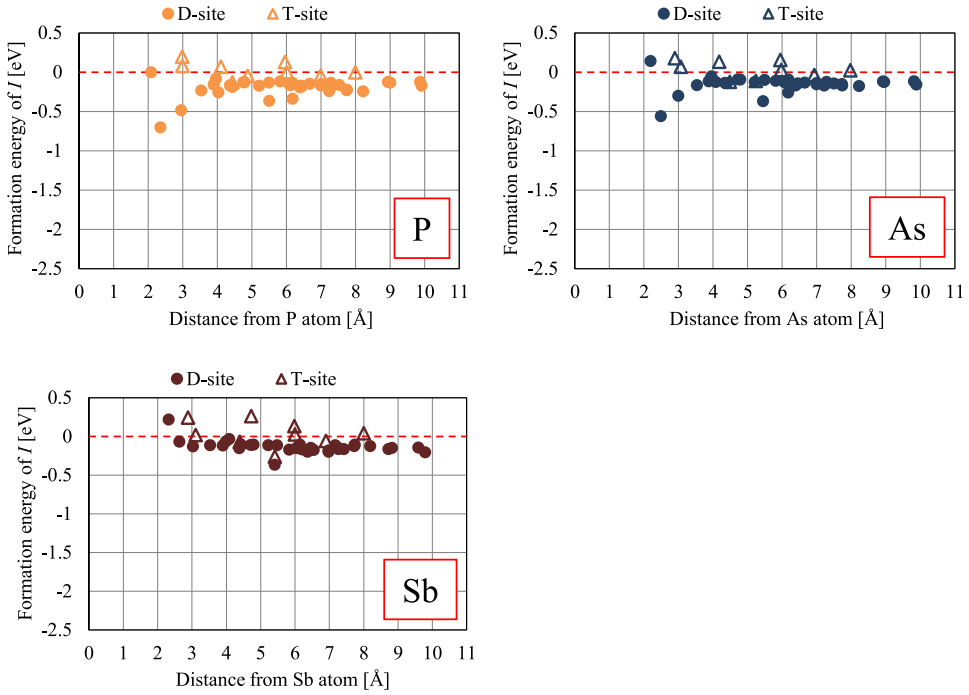

Fig. 8. (color online) Dependence of change in I formation energy (ΔE_f^I) at D-site and T-site compared to that in an undoped Si crystal upon the distance from the n-type dopant atom in the center.

3. Results and discussion

3.1. Formation energy and formation entropy of V *and* I *in the area of influence of dopant atoms in Si*

Figs. 5(a), (b) and (c) plot the dependence of the change in V formation energy (ΔE_f^V) compared to that in a perfect Si crystal on the distance from a p-type, neutral, and n-type dopant atom. Tl and Sb atoms moved to the split vacancy positions during geometry optimization when V is initially set at 1st neighboring site. It is found that the impact of neutral dopants is limited up to 3rd neighboring sites. This result indicates that the strain impact of neutral dopants on the E_f of V is very local. For n- and p-type dopants, the impact on the E_f of V reaches to 12th site and probably also beyond. For larger dopant atoms than Si, the compressive strain effect reduces the E_f of V and can be observed at 2nd, 5th and 8th sites in Si zigzag bond including dopant atom on one {110} plane [10]. The difference of formation energies of V at 6th(a) and at 6th(b) sites is very small.

Fig. 6 plots the dependence of the change in I formation energy (ΔE_f^I) at the D-site and the T-site compared to that in an undoped Si

Table 4
Calculated formation entropies S_f^I of free I, S_f^V of free V, $S_f^{I\ (doped)}$ of I at 1st neighboring site from B and C atoms, and $S_f^{V\ (doped)}$ of V at 1st neighboring site from Sn, P, and As atoms. k_B is the Boltzmann constant.

Dopant	Point defect	$S^{I,V}/k_B$, $S_f^{I,V\ (doped)}/k_B$
–	I	6.61 7.62 (Exp.[14])
-	V	8.71 8.95 (Exp.[14])
B	I	3.63
C	I	5.33
Sn	V	5.65
P	V	1.59
As	V	2.94

crystal upon the distance from the p-type dopant. It was found that E_f^I at the T-site is lower than that at the D-site around p-type dopant atoms. Most of the I originally set at a D-site moved to a T-site during geometry optimization. This is probably due to the direct exchange of an electron from I at the D-site to the acceptor atom, followed by the movement of the positively charged I to a T-site to reduce the number of chemical bonds. The formation energy of I at 4th(a) of T-site is about 0.2 eV smaller than that at 4th(b) of T-site independently of the type of p-type dopant atom. This result indicates that the impact of dopant is determined not only by the distance from the dopant but also by the atomic configuration. It can be also confirmed that the impact of p-type dopants on the formation of I at T-site goes beyond 10 Å from the dopant atom. The maximum distances of Coulomb interaction from p-type dopant atoms to I at T-site will be discussed in Section 3.3.

Fig. 7 plots the dependence of the change in I formation energy (ΔE_f^I) at the D-site and the T-site compared to that in an undoped Si crystal upon the distance from the neutral dopant atom. It was found that E_f^I decreases around a C atom while it remains constant around Ge and Sn atoms. For neutral dopants, E_f^I is determined mainly by the local strain around the dopant atom. The tensile strain around a C atom facilitates to I formation. At the 0th site, the configuration of the [110] C-I dumbbell changed to that of the [100] C-I dumbbell during geometry optimization. The impact of neutral dopants on the formation of I falls well within 10 Å from the dopant atom.

Fig. 8 plots the dependence of the change in I formation energy (ΔE_f^I) at the D-site and the T-site compared to that in an undoped Si crystal upon the distance from the n-type dopant atom. It was found that E_f^I at D-site decreases around P and As atoms while it remains constant around Sb atoms. The tensile strain around P and As atoms facilitates I formation at the D-site. The impact of n-type dopants on the formation of I almost falls within 10 Å from the dopant atom.

Table 4 summarizes the calculated formation entropies S_f^I of free I, S_f^V of free V, $S_f^{I\ (doped)}$ of I at 1st neighboring site from B and C atoms, and $S_f^{V\ (doped)}$ of V at 1st neighboring site from Sn, P and As atoms. It is found that the S_f of I and V in perfect Si agrees well with the experimental values [14]. The B, C atoms binding to I at the 1st site and Sn, P, As atoms binding to V at the 1st site reduce $S_f^{V,I\ (doped)}$ similarly to an interstitial oxygen (O_i) atom binding to V in Si [16]. In case of smaller impacts of dopant atoms, such as vacancy around B and C atoms, self-interstitial around Sn, P, As atoms, the change of formation entropy is probably rather small as we have confirmed for the case of the O_i atom [16].

3.2. Thermal equilibrium concentrations of intrinsic point defects in heavily B, C, Sn, P, and As doped Si

In this section, we evaluate the thermal equilibrium concentrations of trapped and total point defects as a function of the concentrations of B, C, Sn, P and As in Si crystal. Here, we define the "total V or I ($C_{V,I}^{eq,tot}$)" as the sum of free V or I ($C_{V,I}^{eq,free}$) and V or I trapped by the dopants ($C_{V,I}^{eq,trapped}$). The thermal equilibrium concentrations of trapped V and I will change due to the change in the formation energies and formation entropies of the intrinsic point defects around dopant atoms, depending on the concentration and type of dopant atoms. The trapped and total equilibrium V and I concentrations can be written as [17]:

$$\begin{aligned} C_{V,I}^{eq,tot} &= C_{V,I}^{eq,free} + C_{V,I}^{eq,trapped} \\ &= C_{V,I,site}\left[1 - (1 + \sum_{i=1}^{N} Z_i)\frac{C_D}{C_{Si}}\right]\exp(\frac{S_f^{V,I}}{k_B})\exp(-\frac{E_f^{V,I}}{k_BT}) \\ &\quad + C_D \sum_{i=1}^{N} Z_i \exp(\frac{S_f^{V_iI_i(doped)}}{k_B})\exp(-\frac{E_f^{V_iI_i(doped)}}{k_BT}) \\ &= \exp(-\frac{E_f^{V,I}}{k_BT})\left\{C_{V,I,site}\left[1 - (1 + \sum_{i=1}^{N} Z_i)\frac{C_D}{C_{Si}}\right]\exp(\frac{S_f^{V,I}}{k_B})\right. \\ &\quad \left. + C_D \sum_{i=1}^{N} Z_i \exp(\frac{S_f^{V_iI_i(doped)}}{k_B})\exp(\frac{E_f^{V,I} - E_f^{V_iI_i(doped)}}{k_BT})\right\}. \end{aligned} \quad (3)$$

Here, $C_{V,\ site} = 5\times10^{22}$ cm^{-3} is the number of possible V sites per unit volume, which equals the number of Si atoms per unit volume, C_{Si}. $C_{I\text{-}site} = 3\times10^{23}$ cm^{-3} and 5×10^{22} cm^{-3} are the numbers of I at D-sites and T-sites per unit volume, respectively. $S_f^{V,I}$ and $E_f^{V,I}$ are the formation entropy and energy of V and I for intrinsic Si, respectively. k_B is the Boltzmann constant, and T is temperature. Z_i is the coordination number at the i-th site around the dopant as summarized in Tables 1–3. C_D is the dopant concentration and $S_f^{V_iI_i(doped)}$ and $E_f^{V_iI_i(doped)}$ correspond to the formation entropy and energy, respectively, of V and I at the i-th site from the dopant atom. $E_f^{V,I} - E_f^{V_iI_i(doped)}$ in the third row of Eq. (3) is the change in the formation energies of V and I around the dopant atom compared to the intrinsic value.

Here, we assumed for simplicity that (1) the experimentally determined formation energies and entropies of point defects in intrinsic Si [13] can be used, and (2) the calculated changes in the formation energies of intrinsic point defects around dopants compared to the intrinsic Si values, *i.e.*, $E_f^V - E_f^{V_i(doped)}$ and $E_f^I - E_f^{I_i(doped)}$ in Figs. 5–8 can be used. We also assumed that the changes of formation entropy $S_f^{V,I} - S_f^{V_iI_i(doped)}$ of I at 1st neighboring site of C, and V at 1st neighboring site of Sn, P, and As, are the calculated ones. For B atom, we used the same value of S_f^I at 1st neighboring site to I up to 4th T-site as the E_f^I is rather decreased up to 4th T-site as shown in Fig. 6.

Fig. 9 shows the calculated dependence of $C_{V,I}^{eq,trapped}$ and its ratio to $C_{V,I}^{eq,tot}$ ($C_{V,I}^{eq,trapped}/C_{V,I}^{eq,tot}$) for V and I upon the temperature and the concentrations of B, C, Sn, P, and As in Si. From this figure, we obtained expressions of $C_{V,I}^{eq,trapped}$ and $C_{V,I}^{eq,tot}$ for V and I as summarized in Tables 5, 6, respectively.

In order to evaluate the usefulness of the data in Fig. 9 and in Table 5, we attempt to explain the experimental results [14] of void sizes in P and As doped Si and the so-called "Voronkov criterion [24]" in B and C doped Si. Fig. 10 plots the calculated dependence of $C_V^{eq,tot}(T_m)$-$C_I^{eq,tot}(T_m)$ at the melting temperature T_m upon the concentrations of B, C, Sn, P, and As atoms. The parameters of thermal equilibrium V and I concentrations proposed by Nakamura *et al.* [13], $C_V^{eq} = 3.8490\times10^{26}\ \exp(3.94\ \text{eV}/k_BT)$ cm^{-3} and $C_I^{eq} = 6.1166\times10^{26}\ \exp(4.05\ \text{eV}/\ k_BT)$ cm^{-3}, are used for intrinsic Si. The solid lines indicate the results obtained with taking the decrease of S_f into account while the dotted lines indicate the results obtained with neglecting the change of S_f. The experimental results of void size in heavily P and As doped Si are also plotted. It is obvious that the calculated solid lines for P and As well explain the void size quantitatively. The "Voronkov criterion" $(v/G)_0$ can be written as [24]

$$(v/G)_0 = \frac{C_I^{eq}(T_m)D_I(T_m)(E + Q_I) - C_V^{eq}(T_m)D_V(T_m)(E + Q_V)}{k(T_m)^2(C_V(T_m) - C_I(T_m))}, \quad \text{with} \quad E = \frac{E_f^I + E_f^V}{2}. \quad (4)$$

Here, C_I and C_I^{eq} and C_V and C_V^{eq} are the actual and the thermal

equilibrium I and V concentrations, respectively. D_I and D_V are the diffusivities of I and V, respectively. Q_I and $Q_V$are the reduced heat of transport defined as the heat flux per unit flux of I and V atoms in the absence of a temperature gradient, respectively. We assume in case of heavy doping that (1) (i= I or V), and (2) D_I and D_V are not affected by dopant atoms. Fig. 11 plots the dependence on dopant concentration of $(v/G)_0$ normalized with respect to the intrinsic value. The parameters of thermal equilibrium V and I concentrations, diffusion constants of V and I, D_V =3.5071×10^{-4} exp(0.3 eV/k_BT) cm^{2}s^{-1} and D_I =2.4447×10^{-1} exp(0.9 eV/ k_BT) cm^{2}s^{-1}, and the reduced heat of transport of V and I, Q_V=0 and Q_I=1.013 eV, proposed by Nakamura *et al.* [13] are again used for intrinsic Si. The open circles in the figures for C and B doping are the experimental results [14]. It is found that the calculated results for heavy B and C doping agree well with the experimental results.

It is well known that the oxygen precipitation is enhanced by B and C doping [19] while it is suppressed by P and As doping [20,21]. From the viewpoint of binding with intrinsic point defects, our simulation results showed that B and C (P and As) atoms become effective sinks of I (V) below the temperature of grown-in defect formation. Our results well explain not only their impacts to Voronkov criterion and void formation but also their impact to oxygen precipitation. That is, by

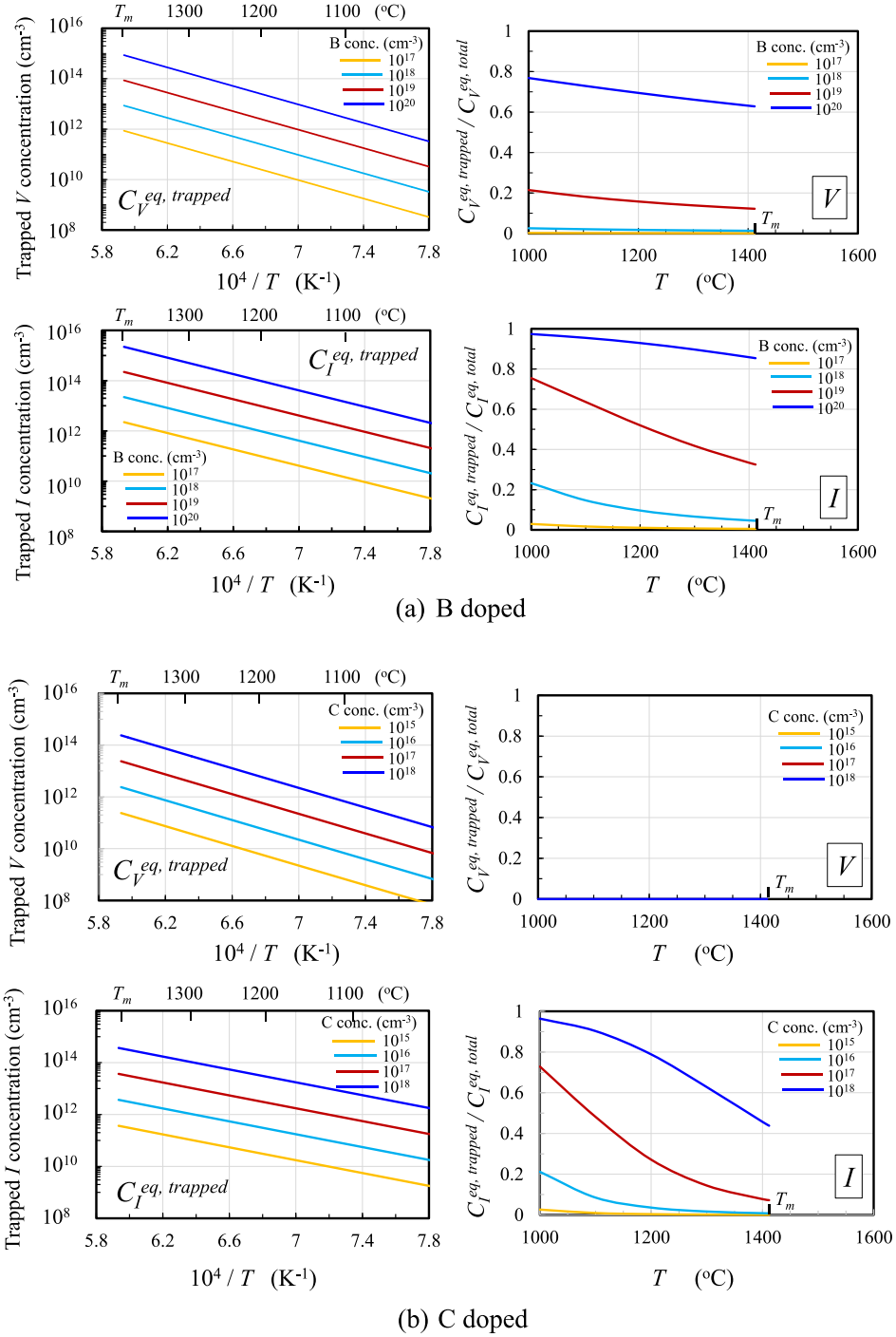

Fig. 9. (color online) Calculated dependence of trapped V/I equilibrium concentration and its ratio to the total thermal equilibrium concentration of V and I upon the temperature and the concentrations of (a) B, (b) C, (c) Sn, (d) P and (e) As in Si crystal.

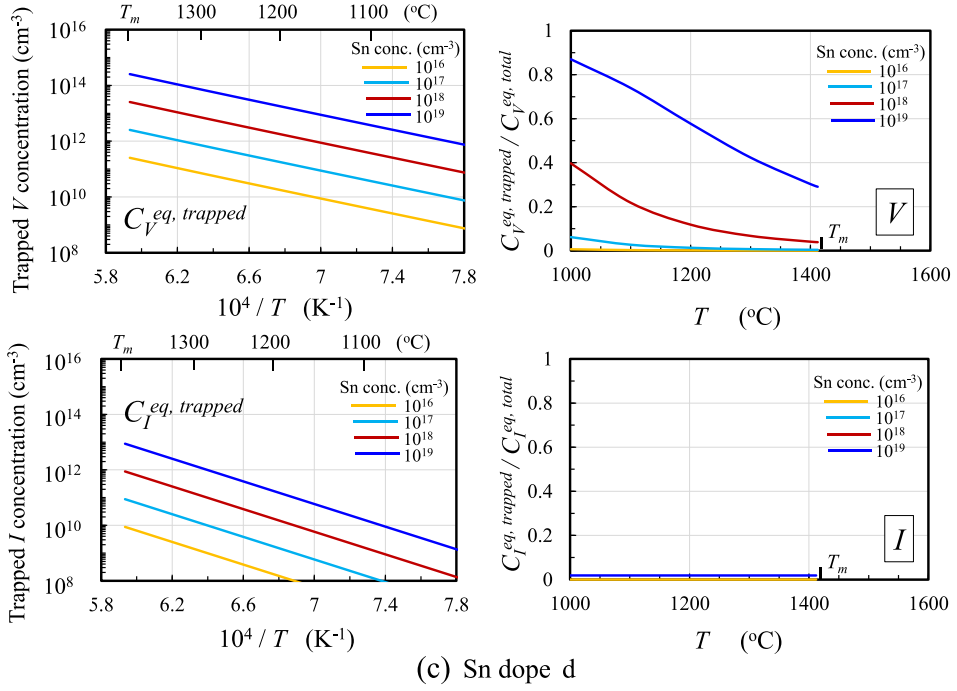

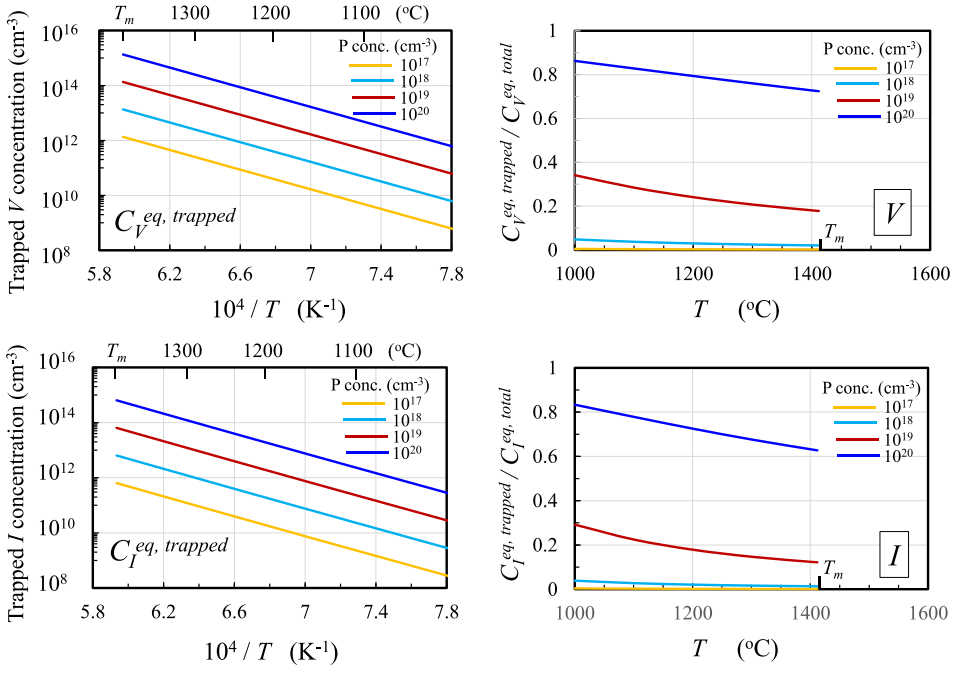

Fig. 9. (*continued*)

means of B and C doping, oxygen precipitation is enhanced as they become effective sinks of emitted *I* by growing oxide precipitates to reduce the local compressive strain. On the other hand, by means of P and As doping, oxygen precipitation is suppressed as they become effective sinks of *V* which should be absorbed by growing oxide precipitates to reduce the local compressive strain.

In summary, the data in Fig. 9 and in Table 5 obtained in the present work well explain the experimental results related to Si single crystal growth from a melt. The expressions should be useful for the numerical simulations of grown-in defect behavior, and probably also for the modeling of oxygen precipitation and dopant diffusion in Si.

3.3. Maximum distances of Coulomb interaction from p (n)-type dopant atoms to I *(V)*

In this section, we have investigated the maximum distances of Coulomb interaction from p-type dopant atoms to *I* and n-type dopant atoms to *V*. As shown in Figs. 5 and 6, the E_f^V of *V* at 12th site from n-type dopant and the E_f^I of *I* at 8th of T-site from n-type dopant atoms are still decreasing by the electrical effect. Rectangular models of 128, 192, 256, and 320 atoms were prepared by 2, 3, 4, and 5 times of 64-atom cubic cell elongated in the [100] direction. Figs. 12(a) and (b) show the calculated formation energies of *V* and *I* as a function of the

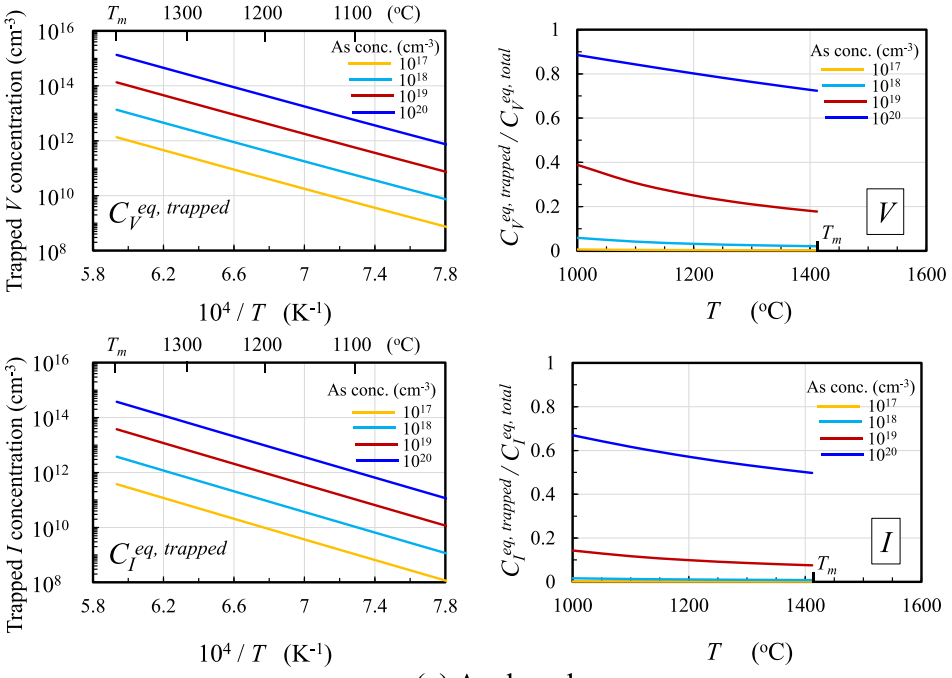

(e) As doped

Fig. 9. (*continued*)

Table 5
Expressions of thermal equilibrium concentrations of trapped V and I, $C_{V,I}^{eq,\ trapped} = C_o \exp(E_f/k_BT)$ (cm^{-3}), in B, C, Sn, P, and As doped Si.

Dopant	$C_V^{eq,\ trapped}$		$C_I^{eq,\ trapped}$	
	C_o (cm^{-3})	E_f (eV)	C_o (cm^{-3})	E_f (eV)
B	6.57×10^5 [B]	3.64	9.42×10^4 [B]	3.22
C	4.43×10^5 [C]	3.77	8.42×10^3 [C]	2.47
Sn	2.74×10^3 [Sn]	2.69	1.13×10^6 [Sn]	4.05
P	5.57×10^5 [P]	3.55	2.90×10^5 [P]	3.57
As	2.97×10^5 [As]	3.47	5.37×10^5 [As]	3.73

Table 6
Expressions of thermal equilibrium concentrations of total V and I, $C_{V,I}^{eq,\ tot} = C_o \exp(E_f/k_BT)$ (cm^{-3}), in B, C, Sn, P, and As doped Si.

Dopant	Dopant Conc. (cm^{-3})	$C_V^{eq,\ tot}$		$C_I^{eq,\ tot}$	
		C_o (cm^{-3})	E_f (eV)	C_o (cm^{-3})	E_f (eV)
B	1×10^{18}	3.76×10^{26}	3.94	3.33×10^{26}	3.96
	1×10^{19}	3.07×10^{26}	3.90	4.00×10^{25}	3.60
	1×10^{20}	1.95×10^{26}	3.73	1.65×10^{25}	3.28
C	1×10^{16}	3.85×10^{26}	3.94	3.19×10^{26}	3.96
	1×10^{17}	3.85×10^{26}	3.94	1.67×10^{25}	3.53
	1×10^{18}	3.85×10^{26}	3.94	2.17×10^{23}	2.83
Sn	1×10^{17}	3.26×10^{26}	3.91	6.12×10^{26}	4.05
	1×10^{18}	1.01×10^{26}	3.75	6.12×10^{26}	4.05
	1×10^{19}	2.91×10^{24}	3.20	6.12×10^{26}	4.05
P	1×10^{18}	3.61×10^{26}	3.93	5.74×10^{26}	4.04
	1×10^{19}	2.34×10^{26}	3.84	3.56×10^{26}	3.96
	1×10^{20}	1.32×10^{24}	3.63	1.12×10^{26}	3.70
As	1×10^{18}	3.49×10^{26}	3.92	6.02×10^{26}	4.05
	1×10^{19}	1.88×10^{26}	3.81	5.16×10^{26}	4.02
	1×10^{20}	7.67×10^{25}	3.55	2.72×10^{26}	3.87
–	0	3.85×10^{26}	3.94	6.12×10^{26}	4.05

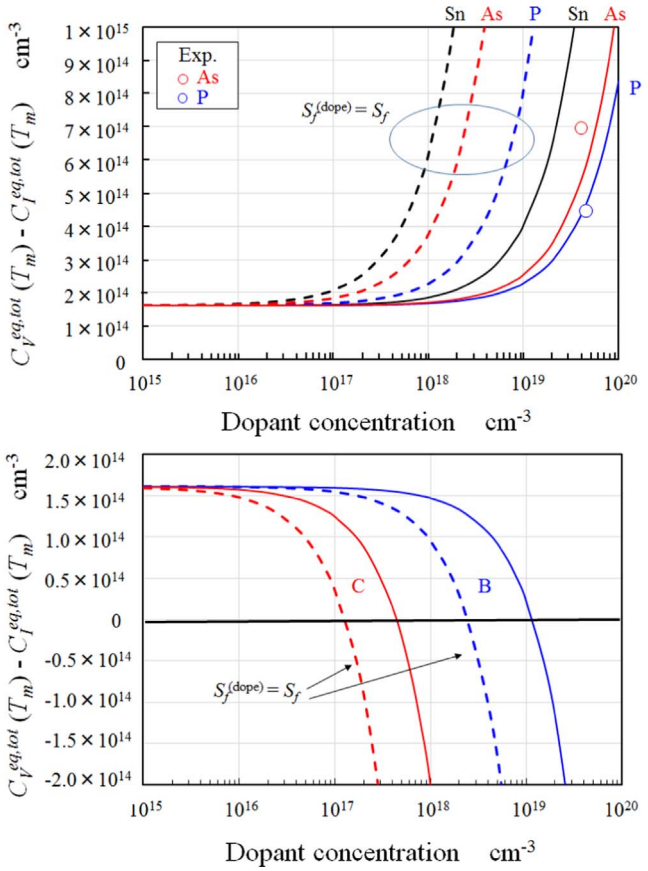

Fig. 10. (color online) Calculated dependence of the difference between V and I equilibrium concentrations at melting temperature of Si upon dopant concentration. Parameters proposed by Nakamura et al. [13] are used. Open circles in figures for P and As doping are experimental results [14].

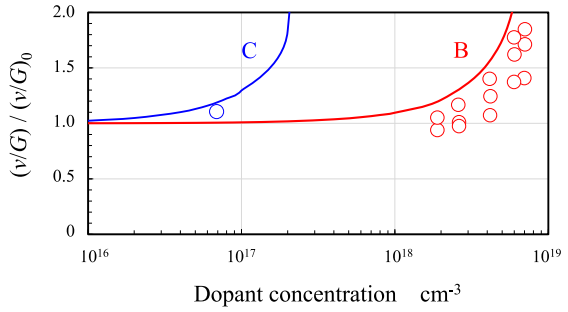

Fig. 11. (color online) Calculated dependence of critical $(v/G)_0$ normalized by intrinsic value upon dopant concentration using the parameters proposed by Nakamura et al. [13]. Open circles in figures for B and C doping are experimental results [14].

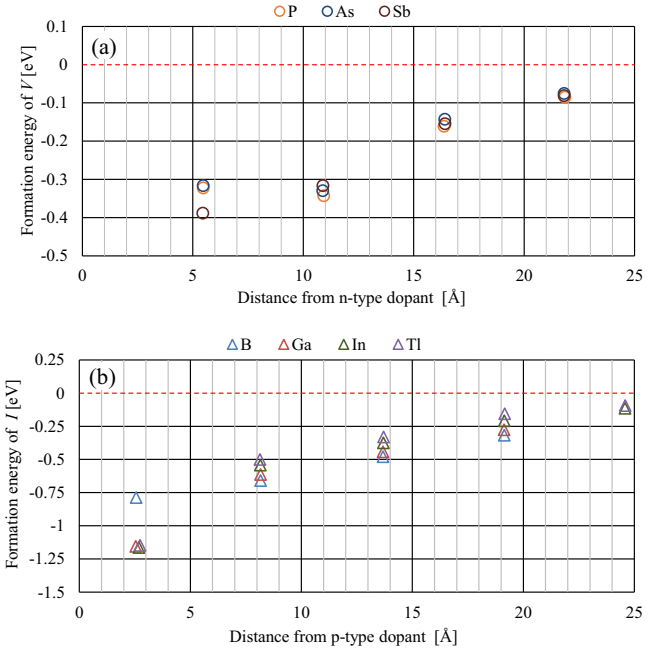

Fig. 12. (color online) Calculated formation energies of V and I as a function of the distance from (a) n-type dopant and (b) p-type dopant atom.

distance from the n-type dopant and p-type dopant atom, respectively. It is found that the Coulomb interaction reaches approximately 30 Å from dopant atoms. It is interesting that the strength of Coulomb interaction of p-type dopant to I is in the order of B > Ga > In > Tl. This result can be understood as telling that the order is the same as that of their electronegativity.

4. Conclusion

We have evaluated the thermal equilibrium concentrations of intrinsic point defects in heavily doped Si crystals. DFT calculations were performed to obtain the formation energy (E_f) of the uncharged V and I at all sites in a 64-atom supercell around the substitutional p-type (B, Ga, In, and Tl), neutral (C, Ge, and Sn) and n-type (P, As, and Sb) dopant atoms. The formation (vibration) entropies (S_f) of free I, V and I, V at 1st neighboring site from B, C, Sn, P and As atoms were also calculated with the linear response method.

The thermal equilibrium concentrations of trapped and total intrinsic point defects (sum of free I or V and I or V trapped with dopant atoms) in heavily B, C, Sn, P or As doped Si were obtained. The experimental results for the so-called “Voronkov criterion” in B and C doped Si, and also the void sizes in P and As doped Si crystals are well explained. The expressions obtained in the present work are useful for the numerical simulation of grown-in defect behavior, and probably also for the modeling of oxygen precipitation and dopant diffusion in Si.

DFT calculations also showed that Coulomb interaction reaches approximately 30 Å from p (n)-type dopant atoms to I (V) in Si.

Acknowledgements

This work was partially supported by JSPS KAKENHI grant Number 25390069.

References

[1] T. Abe, H. Harada, J. Chikawa, Mat. Res. Soc. Proc 14 (1983) 1.
[2] E. Dornberger, D. Graef, M. Suhren, U. Lambert, P. Wagner, F. Dupret, W. von Ammon, J. Cryst. Growth **180** (1997) 343.
[3] K., Nakamura, R., Suewaka, T., Saishoji, J. Tomioka, *Proceedings of the Forum on the Science and Technology of Silicon Materials 2003*, 2003, p. 161 and references therein.
[4] W. Sugimura, T. Ono, S. Umeno, M. Hourai, K. Sueoka, ECS Transactions 2 (2006) 95.
[5] T. Abe, J. Cryst. Growth 334 (2011) 4.
[6] J. Vanhellemont, X. Zhang, W. Xu, J. Chen, X. Ma, D. Yang, J. Appl. Phys. 108 (2010) 123501.
[7] K. Sueoka, M. Yonemura, M. Akatsuka, H. Katahama, T. Ono, E. Asayama, ECS Proceedings 99-1 (1999) 253.
[8] H.-J. Gossmann, T.E. Haynes, P.A. Stolk, D.C. Jacobson, G.H. Gilmer, J.M. Poate, H.S. Luftman, T.K. Mogi, M.O. Thompson, Appl. Phys. Lett. 71 (1997) 3862.
[9] S. Mizuo, H. Higuchi, Jpn. J. Appl. Phys. 20 (1981) 739.
[10] S. Ignacio Martin-Bragado, M. Tian, P. Johnson, R. Castrillo, J. Pinacho, Rubio, M. Jaraiz, Nucl. Instr. and Meth. B 253 (2006) 63.
[11] K. Sueoka, E. Kamiyama, J. Vanhellemont, J. Appl. Phys. 114 (2013) 153510 and references therein.
[12] The CASTEP code is available from Dassault Systems Biovia Inc.
[13] D. Vanderbilt, Phys. Rev. B 41 (1990) 7892.
[14] J. Perdew, K. Burke, M. Ernzerhof, Phys. Rev. Lett. 77 (1996) 3865.
[15] G. Kresse, J. Furthmuller, Phys. Rev. B 54 (1996) 11169.
[16] T. Fischer, J. Almlof, J. Phys. Chem. 96 (1992) 9768.
[17] H. Monkhorst, J. Pack, Phys. Rev. B 13 (1976) 5188.
[18] S. Baroni, S. de Gironcoli, A. dal Corso, P. Giannozzi, Rev. Mod. Phys. 73 (2001) 515.
[19] W. Windl, ECS Transactions 3 (2006) 171.
[20] R. Matsutani, K. Sueoka, E. Kamiyama, Phys. Status Solidi C 11 (2014) 1718.
[21] K. Sueoka, K.Nakamura, and J.Vanhellemont, *J. Cryst. Growth*, submitted for publication.
[22] K. Nakamura, T. Saishoji, J. Tomioka, ECS Proceedings**PV** 2002-2 (2002) 554.
[23] V.V. Voronkov, R. Falster, J. Appl. Phys. 86 (1999) 5975.
[24] K. Sueoka, M. Akatsuka, M. Yonemura, T. Ono, E. Asayama, Y. Koike, S. Sadamitsu, Solid State Phenomena **82-84** (2002) 49.
[25] H. Tsuya, Y. Kondo, M. Kanamori, Jpn. J. Appl. Phys. 22 (1983) L16.